Highly efficient Cas9-mediated gene drive for population modification of the malaria vector mosquito *Anopheles stephensi*

Valentino M. Gantz[a,1], Nijole Jasinskiene[b,1], Olga Tatarenkova[b], Aniko Fazekas[b], Vanessa M. Macias[b], Ethan Bier[a,2], and Anthony A. James[b,c,2]

[a]Section of Cell and Developmental Biology, University of California, San Diego, La Jolla, CA 92093-0349; [b]Department of Molecular Biology and Biochemistry, University of California, Irvine, CA 92697-3900; and [c]Department of Microbiology and Molecular Genetics, School of Medicine, University of California, Irvine, CA 92697-4500

Contributed by Anthony A. James, October 26, 2015 (sent for review October 11, 2015; reviewed by Malcolm Fraser and Marcelo Jacobs-Lorena)

Genetic engineering technologies can be used both to create transgenic mosquitoes carrying antipathogen effector genes targeting human malaria parasites and to generate gene-drive systems capable of introgressing the genes throughout wild vector populations. We developed a highly effective autonomous Clustered Regularly Interspaced Short Palindromic Repeats (CRISPR)-associated protein 9 (Cas9)-mediated gene-drive system in the Asian malaria vector *Anopheles stephensi*, adapted from the mutagenic chain reaction (MCR). This specific system results in progeny of males and females derived from transgenic males exhibiting a high frequency of germ-line gene conversion consistent with homology-directed repair (HDR). This system copies an ∼17-kb construct from its site of insertion to its homologous chromosome in a faithful, site-specific manner. Dual anti-*Plasmodium falciparum* effector genes, a marker gene, and the autonomous gene-drive components are introgressed into ∼99.5% of the progeny following outcrosses of transgenic lines to wild-type mosquitoes. The effector genes remain transcriptionally inducible upon blood feeding. In contrast to the efficient conversion in individuals expressing Cas9 only in the germ line, males and females derived from transgenic females, which are expected to have drive component molecules in the egg, produce progeny with a high frequency of mutations in the targeted genome sequence, resulting in near-Mendelian inheritance ratios of the transgene. Such mutant alleles result presumably from nonhomologous end-joining (NHEJ) events before the segregation of somatic and germ-line lineages early in development. These data support the design of this system to be active strictly within the germ line. Strains based on this technology could sustain control and elimination as part of the malaria eradication agenda.

Plasmodium falciparum | MCR | eradication | transgenesis | CRISPR

Efforts in the ongoing campaign to eradicate malaria show mixed success. The World Health Organization reports that malaria mortality continues to decrease and estimates that ∼3.3 million lives have been saved since 2001 as a result of using new drugs, personal protection, environmental modification, and other measures (1–3). Although these gains are encouraging, there were still ∼580,000 deaths globally in 2014 (3), a statistic that supports the continued application of proven existing control and treatment methods while highlighting the pressing need for strategic development and deployment of new tools.

Prevention of parasite transmission by vector mosquitoes has always played a major role in malaria control (4, 5). However, the challenges of vector control mirror those of malaria eradication in general and include the heterogeneity and complexity of transmission dynamics and the difficulties in sustaining control practices (6, 7). Genetic approaches that result in altering vector populations in such a way as to eliminate their ability to transmit parasites to humans (population modification) can contribute to sustainable control and elimination by providing barriers to parasite and competent vector reintroduction, and allow resources to be directed to new sites while providing confidence that treated areas will remain malaria-free (5, 7).

We and others are pursuing a population-modification approach that involves the introduction of genes that confer a parasite-resistance phenotype to mosquitoes that otherwise would be fully capable of transmitting the pathogens (8–13). The expectation is that the introgression of such an effector gene at a high enough frequency in a vector population would decrease or eliminate transmission and result in measurable impacts on morbidity and mortality (14). Critical to this approach are the development of a gene that confers resistance to the transmission of the parasites, transgenesis tools for introducing the genes into mosquito strains, and a mechanism to spread the genes at epidemiologically significant rates into the target populations. Working with *Anopheles stephensi*, a vector of malaria in the Indian subcontinent (15), we now have demonstrated proof of principle for all of these components.

An. stephensi is both an established and emerging malaria vector. It is estimated to be responsible for ∼12% of all transmission in India, mostly in urban settings, accounting for a total of ∼106,000 clinical cases in 2014 (3, 16–18), and also may be responsible for recent epidemic outbreaks in Africa (19). Laboratory strains of *An.*

Significance

Malaria continues to impose enormous health and economic burdens on the developing world. Novel technologies proposed to reduce the impact of the disease include the introgression of parasite-resistance genes into mosquito populations, thereby modifying the ability of the vector to transmit the pathogens. Such genes have been developed for the human malaria parasite *Plasmodium falciparum*. Here we provide evidence for a highly efficient gene-drive system that can spread these antimalarial genes into a target vector population. This system exploits the nuclease activity and target-site specificity of the Clustered Regularly Interspaced Short Palindromic Repeats (CRISPR) system, which, when restricted to the germ line, copies a genetic element from one chromosome to its homolog with ≥98% efficiency while maintaining the transcriptional activity of the genes being introgressed.

Author contributions: V.M.G., N.J., V.M.M., E.B., and A.A.J. designed research; V.M.G., N.J., O.T., A.F., and V.M.M. performed research; V.M.G., N.J., O.T., A.F., V.M.M., E.B., and A.A.J. analyzed data; and V.M.G., N.J., V.M.M., E.B., and A.A.J. wrote the paper.

Reviewers: M.F., University of Notre Dame; and M.J.-L., Johns Hopkins School of Public Health.

Conflict of interest statement: E.B. and V.G. are authors of a patent applied for by the University of California, San Diego that relates to the mutagenic chain reaction.

Freely available online through the PNAS open access option.

[1]V.M.G. and N.J. contributed equally to this work.

[2]To whom correspondence may be addressed. Email: ebier@ucsd.edu or aajames@uci.edu.

This article contains supporting information online at www.pnas.org/lookup/suppl/doi:10.1073/pnas.1521077112/-/DCSupplemental.

stephensi are transformed efficiently with transposable elements facilitating analyses of transgene expression in diverse genomic locations (20). Site-specific integration technologies adapted to this species allow integrations of exogenous DNA into the mosquito genome at locations with little or no impact on fitness (11, 21). Furthermore, a dual antiparasite effector gene was developed based on the single-chain antibodies (scFvs) m1C3 and m2A10 that target the human malaria parasite *Plasmodium falciparum* ookinete protein Chitinase 1 and the circumsporozoite protein (CSP), respectively (10, 22, 23). Transgenic *An. stephensi* adult females expressing m1C3 and m2A10 had no *P. falciparum* sporozoites (the infectious stage of these parasites) in their salivary glands under infection conditions expected in the field, and therefore were incapable of transmitting parasites (11).

Research on mechanisms for introducing antipathogen effector genes into target populations supports a number of approaches, including inundative releases and those based on gene-drive systems (24). Inundative approaches rely on releases of engineered mosquitoes in numbers substantially exceeding those of the local population to drive gene frequencies high enough to have an epidemiological impact. Inundative releases of chemically or radiation-treated insects were successful in population suppression of mosquitoes using sterile insect technologies (25). However, modeling of gene-drive systems, which exceed rates of Mendelian inheritance, shows a more rapid population-level transformation with fewer releases than inundative approaches (24), and this would result in sustainable local malaria elimination at much reduced costs (7).

We show here that a gene-drive system using Clustered Regularly Interspaced Short Palindromic Repeats (CRISPR)-associated protein 9 (Cas9)-mediated homology-directed repair (HDR) adapted from a highly efficient system, mutagenic chain reaction (MCR), developed in the fruit fly *Drosophila melanogaster* (26) drives target-specific gene conversion at ≥99.5% efficiency in transgene heterozygotes of *An. stephensi*. The drive system as designed works in both the male and female germ lines of mosquitoes derived from transgenic males. Cas9-mediated gene targeting also is evident in the somatic cells of embryos derived from transgenic females. The system can carry a relatively large set of genes (~17 kb in length), and these are transcriptionally active following movement. Strains based on this technology could have a major role in sustaining malaria control and elimination as part of the eradication agenda.

Results

Assembly, Microinjection, and Selection of Transgenic Progeny. The structure of the gene-drive plasmid, pAsMCRkh2, is based on a previous autocatalytically propagating element design (26) and targets its insertion into the locus encoding the kynurenine hydroxylase (kynurenine monooxygenase) enzyme (Fig. 1). The target gene is located autosomally on 3L of the *An. stephensi* linkage map (15), and we refer to it as *kynurenine hydroxylase*^{white} (*kh*^{w}) to indicate orthology with a gene in *Aedes aegypti*, which has a recessive white-eye phenotype (27–29). The pAsMCRkh2 construct has the following elements: (*i*) an *An. stephensi* codon-optimized *Cas9* endonuclease-encoding DNA flanked by the putative promoter, 5′- and 3′-end nucleotide sequences of the *An. stephensi vasa* gene (ASTE003241), intended to drive the expression of the nuclease in both male and female germ lines; (*ii*) a putative *An. stephensi U6A* gene (ASTE015697) promoter directing the expression of a guide RNA (gRNA) targeting the *An. stephensi kh*^{w} gene at a site (designated kh2) immediately adjacent to two known mutations in the *Ae. aegypti* orthologous gene that cause visible eye phenotypes (28, 29); (*iii*) a 3xP3-DsRed gene (30), which expresses the DsRed dominant fluorescence marker visible in larval photoreceptors as well as nonpigmented adult eyes (Fig. 2); (*iv*) dual antipathogen effector genes (m2A10-m1C3) targeting *P. falciparum* (10, 11); and (*v*) DNA fragments ~1 kb in length each that are homologous to the *An. stephensi kh*^{w} locus immediately adjacent to the 5′ and 3′ ends of the kh2 target cut site. The resulting plasmid is a total of ~21 kb in length with 16,625 bp comprising the components ("cargo") targeted for insertion at the *An. stephensi kh*^{w} locus.

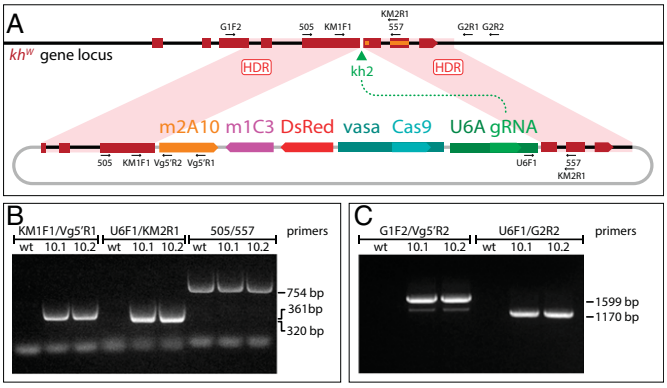

Fig. 1. Site-specific integration into the *An. stephensi kynurenine hydroxylase*^{white} locus of the gene-drive construct AsMCRkh2, carrying antimalarial effector genes. (*A*) Schematic representations of the *kynurenine hydroxylase*^{white} locus and AsMCRkh2 construct. Genes and other features of the AsMCRkh2 construct are not to scale. The dark red boxes represent the eight exons of the endogenous *kh*^{w} gene locus (*Top*) with the direction of transcription indicated by the wedge in exon 8. The black lines represent genomic and intron DNA. The green arrowhead represents the target site of the gRNA, kh2. Labels and arrows indicate names, approximate positions, and directions of oligonucleotide primers used in the study. *kh*^{w} gene sequences corresponding to previously characterized mutations are indicated as an orange rectangle (28) and square (29). The plasmid, AsMCRkh2 (*Bottom*), carries promoter and coding sequences comprising vasa-Cas9 and the U6A-kh2 gRNA genes (U6A gRNA) linked to the dual scFv antibody cassette (m2A10-m1C3) conferring resistance to *P. falciparum* (11) and the dominant eye marker gene (DsRed) inserted between regions of homology (dark red boxes) from the *An. stephensi kh*^{w} locus that directly abut the U6A-kh2 gRNA cut site. The black lines represent *kh*^{w} intron sequences, and the gray lines indicate plasmid DNA sequences. Following gRNA-directed cleavage by the Cas9–kh2 gRNA nuclease complex at the kh2 target site (green arrowhead), homology-directed repair (HDR) leads to precise insertion of the AsMCRkh2 cargo (m2A10-m1C3, DsRed, vasa-Cas9, U6A gRNA) into the genomic *kh*^{w} locus via HDR events somewhere within the regions of homology (pink-shaded quadrilaterals). Plasmid sequences are not integrated. (*B*) Gene amplification analysis confirms integration of the AsMCRkh2 cargo in genomic DNA prepared from the two G_1 male transformants (10.1 and 10.2) that were positive for the DsRed eye-marker phenotype. Both males carry left and right junction fragments of the AsMCRkh2 cargo with the supplied *kh*^{w} regions of homology (KM1F1/Vg5′R1 and U6F1/KM2R1 primer combinations, respectively). An amplicon corresponding to the wild-type *kh*^{w} locus (505/557 primer pairs) confirms that these mosquitoes were heterozygous in some of their cells. Wild-type (wt) control DNA supports amplification only of the wild-type *kh*^{w} locus (505/557 primers). (*C*) Gene amplification analysis confirms site-specific integration of the AsMCRkh2 construct at the *kh*^{w} locus using primers located outside of the genomic sequence included in the AsMCRkh2 cassette (the left integration junction fragment amplified with primers G1F2/Vg5′R2, and the right junction fragment amplified with primers U6F1/G2R2). Wild-type control DNA did not support amplification of these hybrid fragments. Numbers refer to the length in nucleotides of the amplified fragments. Amplicon primary structure was verified by DNA sequencing (*SI Appendix*, Fig. S1).

A total of 680 G_0 wild-type embryos of the Indian strain of *An. stephensi* (15) was injected with a solution containing 100 ng/μL each of the pAsMCRkh2 plasmid, Cas9 protein, Cas9 double-stranded RNAs (dsRNAs), and Ku70 dsRNA. The rationale for including the dsRNAs was to silence expression of the incoming Cas9 gene (dsCas9) carried on the plasmid and to reduce activity of the nonhomologous end-joining (NHEJ) pathway (dsKU70) (31) to favor HDR-mediated insertion of the pAsMCRkh2 cargo. Genomic integration of the transgene was achieved by the coinjected Cas9 protein together with the kh2 gRNA encoded on the

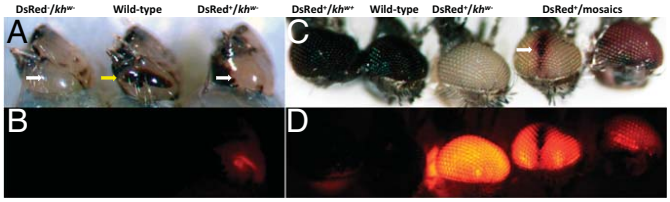

Fig. 2. Larval and adult phenotypes of AsMCRkh2 transgenic *An. stephensi*. Bright-field and fluorescent images of larval (*A* and *B*) and adult (*C* and *D*) eye-color phenotypes. All images are lateral views of the head. Phenotypic descriptions are listed above. White arrows in the larval images indicate the white-eye phenotype, and the yellow arrow indicates the wild-type eye color. Note that all data presented in Tables 1 and 2 for the DsRed$^+$ phenotype are from scoring larvae, not adults. The white arrow in the adult images indicates a patch of wild-type cells in a white-eye background of the left mosaic. The right mosaic exemplifies the colored-eye phenotype.

plasmid. A total of 122 and 129 adult males and females, respectively (37%), survived to the adult stage. Adults were assigned to 22 male-founder and 9 female-founder pools and outcrossed to wild-type adults of the opposite sex. Two males positive for DsRed fluorescence (DsRed$^+$), designated 10.1 and 10.2, were recovered following screening of 25,712 G_1 larvae.

Efficient Autonomous Gene Drive of the AsMCRkh2 Construct. A notable difference in the inheritance patterns of the DsRed marker gene was observed in the G_2 progeny of the 10.1 and 10.2 G_1 males following outcrosses to wild-type females (*SI Appendix*, Table S1). Male 10.1 produced all DsRed$^+$ adult progeny ($n = 14$), whereas male 10.2 produced 44% DsRed$^+$ progeny (57 of 129). Although the number of 10.1 G_2 progeny is too small for statistical analysis, the data are consistent with drive of the DsRed dominant marker gene. However, the line 10.2 DsRed$^+$ ratios were not significantly different from those expected of random Mendelian segregation ($X^2 = 1.744$, df = 1; $P = 0.1866$).

Target-specific integration of the transgene into the *kh*^{w} locus was verified in each of the G_1 founder males by gene amplification using oligonucleotide primers complementary to DNA within the construct and outside the regions of homology included in the construct (Fig. 1 and *SI Appendix*, Table S2). Sequencing of the ends of the diagnostic amplicons spanning both sides of the insertion within the *kh*^{w}-coding region confirmed the structure and precise integrity of the junctions of the transgene and genomic DNAs (*SI Appendix*, Fig. S1).

DsRed$^+$ G_2 males and females derived from 10.1 and 10.2 G_1 founders were outcrossed individually and in batch matings to wild-type mosquitoes, and G_3 larval progeny were scored for DsRed. Extreme non-Mendelian DsRed segregation patterns were evident in both 10.1 and 10.2 G_2 male and female outcrosses (*SI Appendix*, Tables S3 and S4). Line 10.1 yielded 1,321 (99.7%) DsRed$^+$ and 7 DsRed$^-$ G_3 larvae, whereas 10.2 produced 4,631 (99.2%) DsRed$^+$ and 35 DsRed$^-$ G_3 larvae. These highly biased transmission frequencies deviate significantly from the 50% allele inheritance expected of random segregation. Three DsRed$^-$ larvae with white eyes (*kh*$^{w-}$) were recovered from female-founder families, and gene amplification and sequencing confirmed that they have target site-specific deletions in the *kh*^{w} locus consistent with Cas9-mediated NHEJ (*SI Appendix*, Fig. S2).

Non-Mendelian segregation patterns consistent with gene drive were also seen in the eye-color phenotypes of lines 10.1 and 10.2 G_3 larvae that survived to adults (Table 1 and *SI Appendix*, Tables S5 and S6). Three major adult phenotypes consistent with HDR were seen: mosquitoes positive for DsRed with an otherwise wild-type eye color (DsRed$^+$/*kh*$^{w+}$), mosquitoes positive for DsRed with a white eye color (DsRed$^+$/*kh*$^{w-}$), and mosquitoes positive for DsRed with mosaicism evident in the eyes (DsRed$^+$/mosaic) (Fig. 2). Additionally, a number of G_3 progeny from female-founder families scored as DsRed$^+$/*kh*$^{w-}$ phenotype (positive for DsRed/white eye color) were modified by eye coloring ("coloring"; *SI Appendix*, Table S6). This coloring is consistent with partial cell-nonautonomous rescue of the white-eye phenotype by wild-type expression of the gene in a somatic location other than the eye or a hypomorphic allele generated by NHEJ. The frequency of this coloring phenotype in the 10 families in which it was explicitly scored varied from 5 to 32%, with an average of ~17%. The non-drive phenotypic classes were mosquitoes negative for DsRed with a wild-type eye color (DsRed$^-$/*kh*$^{w+}$) and the rare mosquitoes negative for DsRed with a white eye color (DsRed$^-$/*kh*$^{w-}$) seen in the larvae (Fig. 2 and Table 1).

The numerical summaries of the G_3 adult phenotypes confirm the non-Mendelian segregation patterns consistent with highly efficient gene drive. Male 10.1 and 10.2 DsRed$^+$/*kh*$^{w+}$ single founders and those batch-mated to wild-type females produced a total of 2,113 G_3 progeny, 98.9% (2,091) of which were DsRed$^+$ (Table 1). None of the progeny derived from males had white or mosaic eyes, indicating that these individuals were heterozygous for the gene-drive construct. Individual DsRed$^+$/*kh*$^{w+}$ 10.1 and 10.2 female founders produced a total of 1,781 progeny, of which 1,778 (99.8%) were DsRed$^+$. Notably, 5 of 7 of the 10.1 G_2 outcrosses and all 15 of the 10.2 female outcrosses had 100% DsRed$^+$ G_3 progeny (*SI Appendix*, Tables S5 and S6). The combined data from both male and female founders total 3,869 DsRed$^+$ G_3 progeny and 25 wild-type G_3 progeny, amounting to ~99.5% efficiency of inheritance of the cargo facilitated by a 98.8%

Table 1. Summary of G_3 adult phenotypes of lines 10.1 and 10.2 G_2 outcrosses to wild-type mosquitoes

		Adult phenotypes*									
		G_3 males					G_3 females				
Line	Founder	DsRed$^+$/*kh*$^{w+}$	DsRed$^+$/*kh*$^{w-}$	DsRed$^+$/mosaic	DsRed$^-$/*kh*$^{w+}$	DsRed$^-$/*kh*$^{w-}$	DsRed$^+$/*kh*$^{w+}$	DsRed$^+$/*kh*$^{w-}$	DsRed$^+$/mosaic	DsRed$^-$/*kh*$^{w+}$	DsRed$^-$/*kh*$^{w-}$
10.1	G_2 ♂†	414	—	—	3	—	419	—	—	—	—
	G_2 ♀†	—	155	25	1	—	—	180	27	2	—
10.2	G_2 ♂‡	663	—	—	8	3	595	—	—	8	—
	G_2 ♀†	—	597	130	—	—	—	585	79	—	—
Subtotal		1,077	752	155	12	3	1,014	765	106	8	—
Total			1,984§		15§			1,885§		10§	

*Shaded cells are all G_3 progeny positive for DsRed (DsRed$^+$).
†Progeny of single G_2 founders outcrossed to wild-type counterparts.
‡Twenty-seven G_2 males outcrossed to 270 wild-type females.
$^\S X^2$ analyses show significant differences from random segregation.

gene-conversion rate. This latter value is derived from a formula: conversion rate = 2(X − 0.5N)/N, where N is the total number of mosquitoes and X is the number of DsRed-positive individuals, which accounts for the fact that 50% of the progeny would be expected to inherit the transgene by traditional Mendelian segregation (26). These combined data support the conclusion that Cas9-mediated gene conversion resulting from HDR can occur at near-complete efficiency in the germ-line cells of both male and female mosquitoes carrying the AsMCRkh2 cargo.

Remarkably, all but 3 of the 1,781 G_3 progeny from individual DsRed$^+$/kh^{w+} 10.1 and 10.2 female founders had either white or mosaic eyes (DsRed$^+$/kh^{w-} phenotype; Table 1 and *SI Appendix*, Tables S5 and S6). These data show that not only do the progeny derived from phenotypically DsRed$^+$/kh^{w+} female founders outcrossed to wild-type males transmit the gene-drive constructs with high efficiency via the germ line but that the paternally inherited kh^{w+} gene is targeted somatically by the Cas9 nuclease and gRNAs in the zygote and developing embryo, where it is mutagenized by either NHEJ or HDR at a high efficiency (99.8% of adult progeny). In contrast, no DsRed$^+$/kh^{w-} G_3 progeny were recovered from the DsRed$^+$/kh^{w+} male-founder outcrosses. These data support the interpretation that the eggs of transgenic AsMCRkh2 females contain both Cas9 protein and kh2 gRNA. Sex specificity (Cas9 presence in female but not male gametes) of the somatic mutation phenotype is likely conferred by the *vasa* regulatory sequences used for Cas9 expression, and this is consistent with the expression profile of the orthologous *vasa* gene in *Anopheles gambiae* (32).

Maternal Effects Result in Differential Transmission of the pAsMCRkh2 Cargo. DsRed$^+$/kh^{w+} and DsRed$^+$/kh^{w-} 10.1 and 10.2 G_3 males and females were outcrossed separately in batches to wild-type mosquitoes of the appropriate opposite sex and G_4 progeny were scored both as larvae and adults. Larval screening for the DsRed phenotype showed two distinct distributions of the phenotypic classes depending on the history of the lineage. G_4 larval progeny of G_3 males and females derived from G_2 10.1 and 10.2 transgenic males (crosses 5–8; *SI Appendix*, Tables S7 and S8) show a high frequency (98.5%) of DsRed transmission, corresponding to a 96.9% rate of gene conversion. In contrast, a much higher proportion of G_4 larval progeny of G_3 males and females derived from G_2 10.1 and 10.2 transgenic females (crosses 1–4; *SI Appendix*, Tables S7 and S8) appear to have inherited mutations at the kh^w locus instead of gene-conversion events, as evidenced by inheritance ratios of 1.33:1 (936 DsRed$^+$: 703 DsRed$^-$) for the transgene cargo. However, this ratio still deviates from that expected by Mendelian segregation alone ($X^2 = 33.123$, df = 1; $P < 0.0001$). We interpret these results to indicate that the progeny of pAsMCRkh2 females often inherit "indel" mutations presumably generated via the NHEJ pathway in the male-derived kh^w allele. However, the excess of DsRed$^+$ larvae among the progeny is consistent with a fraction of the incoming chromosomes also having been converted by HDR.

The presumed high level of NHEJ in G_4 progeny of DsRed$^+$/kh^{w-} G_3 males and females derived from G_2 10.1 and 10.2 transgenic females (crosses 1–4; *SI Appendix*, Tables S7 and S8) supports the hypothesis that the G_3 parents were at least partially heterozygous for the DsRed cargo component of the transgene and a nonconverted mutant kh^w allele. Genomic DNA prepared from 20 individual male and female DsRed$^+$/kh^{w-} G_3 founder mosquitoes was used with gene-specific primers to amplify the kh2 target portion of the kh^w gene. Diagnostic fragments of 754 bp were seen in each of the samples, indicating that these mosquitoes had chromosomes without the large ∼17-kb transgene cargo inserted into it (*SI Appendix*, Fig. S3). These fragments must include mutant alleles, because the eye phenotype of each mosquito from which the DNA was derived was white (kh^{w-}).

The G_4 progeny of separate batch intercross matings of 10.1 and 10.2 DsRed$^+$ G_3 siblings yielded a combined total of 2,279 DsRed$^+$ and 432 DsRed$^-$ larvae (*SI Appendix*, Table S9). The inheritance ratio, ∼5.3:1 (DsRed$^+$:DsRed$^-$), differs significantly from 3:1 ($X^2 = 118.811$, df = 1; $P < 0.0001$), that expected of an intercross of two parents heterozygous for DsRed$^+$. These data provide further support for the conclusion that some level of HDR continues to occur in the G_3 females derived from G_2 10.1 and 10.2 transgenic females.

The numerical summaries of the G_4 adult phenotypes confirm the strong Cas9-mediated gene drive through both male and female germ lines in individuals derived from wild-type males. Male G_3 10.1 and 10.2 DsRed$^+$/kh^{w+} batch-mated to wild-type females produced a total of 1,471 G_4 progeny, 98.4% (1,447) of which were DsRed$^+$ (Table 2; crosses 6 and 8). As in previous outcrosses of DsRed$^+$ cargo-bearing males, none of the progeny had white or mosaic eyes, indicating that these individuals were heterozygous for the gene-drive construct in somatic tissues. Female G_3 10.1 and 10.2 DsRed$^+$/kh^{w+} batch-mated to wild-type males produced 1,523 adult G_4 progeny, 98.8.% (1,505) of which were DsRed$^+$ (Table 2; crosses 5 and 7). Additionally, 1,500 (99.7%) of the DsRed$^+$ mosquitoes derived from DsRed$^+$/kh^{w+} mothers had white or mosaic/colored eyes, a result consistent with previous outcrosses of this type. The combined data from both DsRed$^+$/kh^{w+} male and female G_3 outcrosses total 2,952 DsRed$^+$ and 42 wild-type G_4 progeny, amounting to ∼98.6% efficiency of inheritance of the cargo and corresponding to a 97.2% rate of gene conversion. These data provide strong support for the conclusion that Cas9-mediated gene drive continues

Table 2. Summary of G_4 adult phenotypes of lines 10.1 and 10.2 G_3 outcrosses to wild-type mosquitoes

G_3 founder (crosses)†	Adult phenotypes*: G_4 males					G_4 females				
	DsRed$^+$/kh^{w+}	DsRed$^+$/kh^{w-}	DsRed$^+$/mosaic	DsRed$^-$/kh^{w+}	DsRed$^-$/kh^{w-}	DsRed$^+$/kh^{w+}	DsRed$^+$/kh^{w-}	DsRed$^+$/mosaic	DsRed$^-$/kh^{w+}	DsRed$^-$/kh^{w-}
DsRed$^+$/kh^{w-} ♀ (1 and 3)	—	46	35	40	44	—	42	53	30	5
DsRed$^+$/kh^{w-} ♂ (2 and 4)	310	—	—	212	—	313	—	—	276	—
DsRed$^+$/kh^{w+} ♀ (5 and 7)	4	443	226	10	1	1	580	251	4	3
DsRed$^+$/kh^{w+} ♂ (6 and 8)	661	—	—	13	—	786	—	—	11	—

*Shaded cells are all G_4 progeny positive for DsRed (DsRed$^+$).
†Crosses are listed in Fig. 3 and *SI Appendix*, Tables S10 and S11.

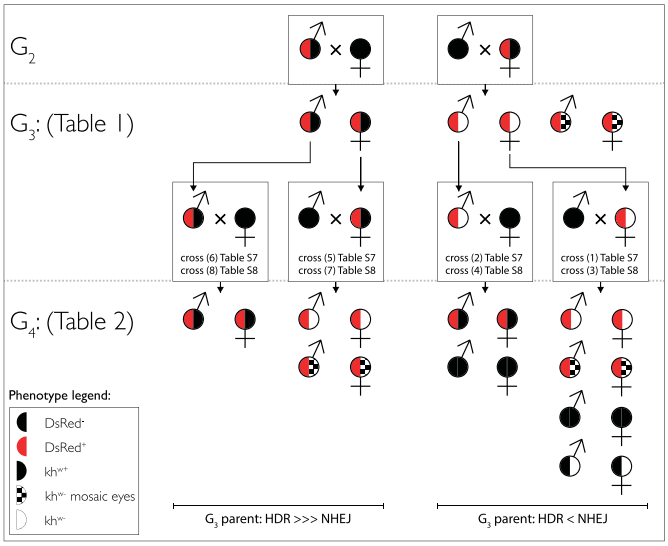

Fig. 3. Phenotypic inheritance patterns of the AsMCRkh2 gene-drive cargo. (*Top*) DsRed-positive G_2 transgenic adult males and females with wild-type eye color (DsRed$^+$/*kh*$^{w+}$, half-red and half-black circles) were outcrossed to wild-type mosquitoes (all-black circles) of the opposite sex. (*Middle*, *Upper*) G_3 progeny resulting from the male outcrosses were predominantly DsRed$^+$/*kh*$^{w+}$ (half-red and half-black circles; Table 1). G_3 progeny resulting from the female outcrosses were predominantly positive for DsRed and had white (DsRed$^+$/*kh*$^{w-}$, half-red and half-white circles) or mosaic eyes (DsRed$^+$/mosaic, half-red and half-checkered white and black circles). (*Middle, Lower*) DsRed$^+$/*kh*$^{w+}$ (half-red and half-black circles) and DsRed$^+$/*kh*$^{w-}$ (half-red and half-white circles) G_3 adult males and females were outcrossed to wild-type mosquitoes (all-black circles) of the opposite sex. Specific crosses and tables for the data are referenced. (*Bottom*) G_4 progeny resulting from outcrosses of DsRed$^+$/*kh*$^{w+}$ G_3 adult males (half-red and half-black circles; crosses 6 and 8) were predominantly DsRed$^+$/*kh*$^{w+}$ (half-red and half-black circles), whereas those from G_3 DsRed$^+$/*kh*$^{w+}$ adult females (half-red and half-black circles; crosses 5 and 7) were predominantly positive for DsRed and had white (DsRed$^+$/*kh*$^{w-}$, half-red and half-white circles) or mosaic eyes (DsRed$^+$/mosaic, half-red and half-checkered white and black circles). In contrast, G_4 progeny resulting from outcrosses of DsRed$^+$/*kh*$^{w-}$ G_3 adult males (crosses 2 and 4) were either DsRed$^+$/*kh*$^{w+}$ (half-red and half-black circles) or DsRed$^-$/*kh*$^{w+}$ (wild-type eye, all-black circles). G_4 progeny derived from female DsRed$^+$/*kh*$^{w-}$ outcrosses (crosses 1 and 3) were also a mix of DsRed$^+$ and DsRed$^-$. Nearly all DsRed$^+$ progeny had white (DsRed$^+$/*kh*$^{w-}$, half-red and half-white circles) or mosaic (DsRed$^+$/mosaic, half-red and half checkered circles) eyes (Table 1). Among the DsRed$^-$ progeny, approximately half had wild-type eyes (all-black circles) and half had white eyes (half-black and half-white circles). Male-derived (G_2 cross) G4 progeny (*Left*) show a bias of HDR over NHEJ, whereas female-derived (G_2 cross) G_4 progeny lines display nearly equal HDR and NHEJ.

to occur efficiently and in a multigenerational fashion in the germ line of these transgenic mosquitoes.

The reduced germ-line transmission of the AsMCRkh2 cargo in G_4 larvae derived from DsRed$^+$/*kh*$^{w-}$ G_3 parents described above also was evident in the adult phenotypes. The ratio (1.27:1) of DsRed$^+$/DsRed$^-$ phenotypes of the corresponding adult G_4 progeny derived from DsRed$^+$/*kh*$^{w-}$ males (Table 2; crosses 2 and 4; *SI Appendix*, Tables S10 and S11) still deviates from that expected by Mendelian segregation alone ($X^2 = 16.404$, df = 1; $P < 0.0001$). Similarly, G_4 adult progeny of DsRed$^+$/*kh*$^{w-}$ females (Table 2; crosses 1 and 3; *SI Appendix*, Tables S10 and S11) had a DsRed$^+$/DsRed$^-$ phenotypic ratio of 1.48:1, also significantly different from that expected solely by Mendelian segregation ($X^2 = 11.014$, df = 1; $P = 0.0009$). However, in contrast to the crosses with male G_3 parents in which all DsRed$^-$ progeny were *kh*$^{w+}$, 41.2% (49/119) of the DsRed$^-$ progeny of G_3 females had white eyes (*kh*$^{w-}$). These data provide further support for the conclusion that Cas9–gRNA complexes perdure in eggs derived from transgenic cargo-bearing females. The relatively fewer number of progeny derived from the DsRed$^+$/*kh*$^{w-}$ females may be indicative of a load associated with this genotype.

The differences and consequences of the maternal effects on gene drive are summarized in Fig. 3. In all cases where the AsMCRkh2 cargo is propagated by outcrossing DsRed$^+$/*kh*$^{w+}$ males to wild-type females, high-frequency DsRed$^+$/*kh*$^{w+}$ progeny are recovered. This inheritance of the cargo is consistent with HDR gene drive and extends through an additional generation. In contrast, propagation of the AsMCRkh2 cargo by outcrossing DsRed$^+$/*kh*$^{w+}$ females to wild-type males produces a high frequency of DsRed$^+$/*kh*$^{w-}$ along with somatic mosaicism. Continued outcrossing of these individuals to wild-type mosquitoes results in progeny inheriting the AsMCRkh2 cargo in ratios approaching Mendelian segregation. Although some degree of gene drive is observed in these mosquitoes, HDR-mediated copying of the AsMCRkh2 cargo is reduced (typically ∼12–25% conversion assayed in larvae and adults; Table 2) relative to crosses in which that construct has been propagated with high fidelity via DsRed$^+$/*kh*$^{w+}$ parents. The most likely explanation for this difference is that in crosses where the AsMCRkh2-bearing parent is female, Cas9 protein is presumably expressed throughout the cytoplasm of the egg, where it may generate indel mutations via NHEJ that disrupt the gRNA cleavage site and thereby preclude subsequent HDR-mediated copying of the cargo in the germline lineages.

The Antipathogen Effector Genes Are Transcriptionally Active. The m1C3 and 2A10 scFvs are under the control of the blood meal-inducible 5′- and 3′-end regulatory elements of the *An. gambiae carboxypeptidase A* (*AgCPA*) and *An. stephensi Vitellogenin 1* (*AsVg1*) genes, respectively (11). Blood meal-induced, tissue-specific accumulations of m1C3 and 2A10 transcripts were observed by RT-PCR analysis of total RNA isolated from G_3 DsRed$^+$/*kh*$^{w-}$ dissected females and whole males (Fig. 4). Midgut and carcass (all tissues except the midguts) were collected from females at 0, 4, 12, 24, and 48 h post blood meal (hPBM). The *AgCPA* promoter driving expression of the m1C3 scFv displays constitutive midgut-specific expression in the absence of a blood meal but increases to a peak at 4 hPBM and falls over the next 2 d, consistent with the endogenous expression profile of the orthologous gene from *An. stephensi* (10). Expression of the 2A10 transgene product by the *AsVg1* promoter shows induction at 12 hPBM with a qualitative maximum at 24 hPBM in carcasses and an earlier induction in the midgut. Because midgut expression is not a characteristic feature of the endogenous gene (33), position effects resulting from the insertion site may contribute to this result. As expected, samples from males show no expression from either transgene. These data support the conclusion that the antipathogen effector genes are transcribed in a blood meal-regulated fashion following Cas9-mediated integration.

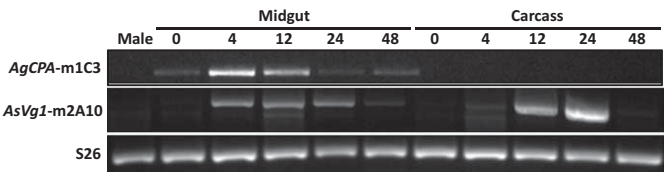

Fig. 4. Expression of m1C3 and m2A10 transcripts in AsMCRkh2 transgenic females. RT-PCR was used to detect m1C3 (*AgCPA*-m1C3) and m2A10 (*AsVg1*-m2A10) transcripts in RNA isolated from homogenates of dissected midguts and the remaining carcasses of mixed heterozygous and homozygous DsRed$^+$ G_3 females at 0 (non–blood-fed), 4, 12, 24, and 48 h post blood meal. Male transgenic mosquitoes were used as negative controls. The *An. stephensi* S26 ribosomal protein transcript was amplified from all samples as a loading control.

Discussion

The data presented here support the following conclusions: (*i*) Cas9-mediated gene drive based on a system adapted from MCR works well in a malaria mosquito, *An. stephensi*; (*ii*) the gene-drive system is target-specific; (*iii*) the system works in the germ line of both males and females; (*iv*) the system is active early in the somatic cells of embryos derived from transgenic females; (*v*) the gene-drive system can carry a relatively large cargo; and (*vi*) the cargo is functional (at the transcriptional level). These results provide the basis for the further development of Cas9-mediated gene-drive technology in sustaining malaria control and elimination as part of the eradication agenda.

The use of both dominant and recessive marker genes for gene-drive function, as well as the choice of promoter for driving the Cas9 activity, has provided a number of insights that can guide the further development of this approach into a functional system for malaria control. The tight linkage of the DsRed marker gene to the anti-pathogen effector scFvs allows the tracking of the malaria-resistance phenotype by monitoring fluorescence in samples of larvae. This is expected to have significant practical value as this technology continues to be developed for the field. Targeting the kh^{w} gene allowed us to monitor the specificity of Cas9-mediated gene conversion and mutagenesis by scoring the white-eye phenotype. Furthermore, the data presented here provide support for the hypothesis that there is a load associated with the white-eye phenotype (homozygous kh^{w-}), so this locus may not be optimal for any strain developed for field applications. Other target sites are available in the *An. stephensi* genome that appear not to have any significant fitness issues (10, 11, 21), and further validation of the technology may make it unnecessary to target loci with recessive visible phenotypes.

The sex-specific expression of Cas9 mediated by the *An. stephensi vasa* ortholog control DNA sequences was highly informative for the design of future autonomous gene-drive systems. Previous transgene analysis of the *An. gambiae vasa* ortholog showed that it is active in both male and female germ-line tissues, and that sex- and tissue-specific enhancer-like sequences could be localized in the promoter and 5′ untranslated regions (5′UTRs) (32). We chose to use the complete promoter and 5′UTR sequences of the *An. stephensi* ortholog in our autonomous construct to maximize the potential for germ-line gene conversion via HDR. This allowed us to discover the effects of pre- and postzygotic activity of the Cas9 nuclease and gRNAs and the impact of HDR and NHEJ on subsequent gene drive and inheritance.

Our data support a model in which the gene drive and inheritance of the transgene cargo are optimized in the progeny of transgenic males whose female parent was wild-type (Fig. 5). Male and female progeny of these males also faithfully transmitted the cargo to their progeny. However, progeny of transgenic males and females whose parent was a transgenic female transmit the cargo in ratios similar to what is expected of Mendelian segregation, although there does appear to be some residual drive. These differences can be understood in terms of a maternal effect of Cas9 expression in the developing embryos. Outcrosses of transgenic male parents to wild-type females result in an embryonic environment in which the eggs lack maternally produced Cas9. Hence, Cas9 expression is restricted to the germ line, where it continues to catalyze high-frequency HDR. In contrast, outcrosses of transgenic female parents to wild-type males produce embryos in which the eggs have active levels of Cas9 and kh2 gRNAs. The wild-type kh^{w} (kh^{w+}) allele contributed by the sperm can be subject to Cas9-mediated activity in pre- and postsyncytial blastoderm nuclei before cellularization and partitioning of the germplasm into posterior cells to form the germ line. This early activity could result in either HDR or NHEJ. Given the initial physical separation of the paternally derived kh^{w+} allele from the maternally derived allele immediately following fertilization, the repair template (the DsRed^{+}, kh^{w-} allele) may be positioned sufficiently far from the Cas9-induced double-stranded break and favor NHEJ. The fact that nearly all progeny from such crosses manifest a white-eye phenotype supports the interpretation that such early-acting mutagenesis occurs at a high frequency. Importantly, once a homologous chromosome has been mutated by NHEJ, key nucleotides required for gRNA recognition will typically be eliminated, thus precluding subsequent HDR-mediated gene conversion in the germ line. This has a dampening effect on drive, and progeny phenotype ratios thus approach Mendelian inheritance. This also explains the rare phenotypes we observed in the female-derived lines.

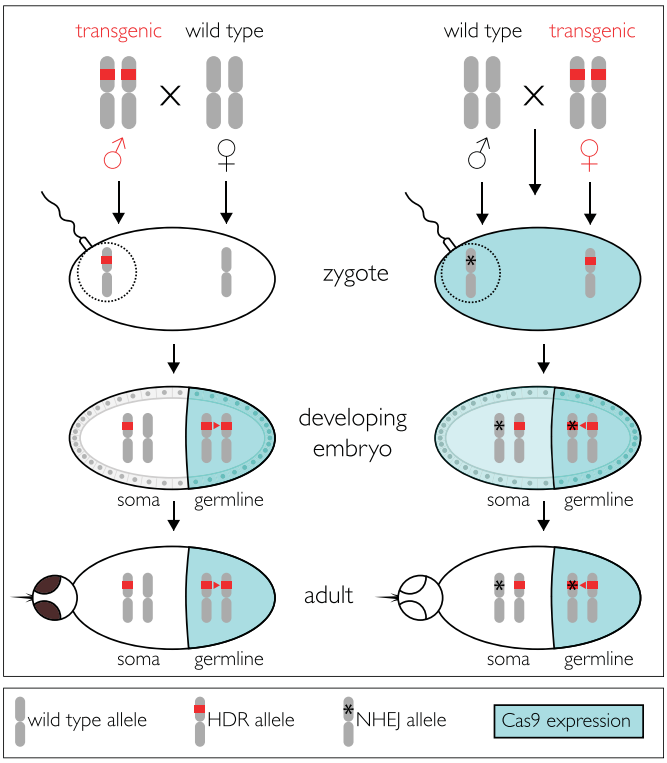

Fig. 5. Model of AsMCRkh2 transgene activity in adult males and females. (*Top*) Schematic representations of the third chromosomes of *An. stephensi*. Transgenic males (*Left*) and females (*Right*) are depicted as being homozygous in the germline for AsMCRkh2 (red bars) and are outcrossed to wild-type mosquitoes of the opposite sex. Zygotes resulting from outcrosses of transgenic males do not have the Cas9 nuclease in the eggs (clear oval), which are derived from wild-type females, and somatic cells remain heterozygous for the AsMCRkh2 transgene. A schematic representation of the sperm attached to the egg and the donated paternal chromosome is represented encircled by the dotted line. *vasa*-mediated expression of Cas9 is restricted to the germ line (colored half-oval) in developing embryos derived from transgenic AsMCRkh2 males, resulting in significant HDR (red arrowhead) that converts the majority of the chromosomes by insertion of the AsMCRkh2 cargo. Adults are phenotypically positive for the dominant reporter gene, DsRed, and wild-type in eye color. In contrast, zygotes resulting from outcrosses of transgenic females have Cas9 nuclease in the eggs (aqua-colored oval) as a result of *vasa*-directed expression in the maternal germ line, and this catalyzes nonhomologous end joining (asterisk) to mutate the paternally derived wild-type chromosome (encircled by the dotted line). Some HDR may occur at this stage, but may be hampered by an initial physical separation of the maternal and paternal chromosomes. Embryos derived from transgenic AsMCRkh2 females also have *vasa*-mediated Cas9 expression restricted to the germ line (colored half-oval), but in addition have the nuclease perduring from the maternal gamete (light-colored half-oval), which can result in adults that are phenotypically positive for the dominant reporter gene, DsRed, and exhibit the white or mosaic eye color. Furthermore, the paternally derived chromosomes mutagenized in the zygotes are resistant to subsequent HDR and insertion of the cargo. Some of the male-derived chromosomes may not be mutagenized, and these can be substrates for HDR. Both options are shown as the asterisk overlying the red bar in the germ line.

Two types of mosaic phenotypes result in those animals where mutagenesis of the kh^w locus is not complete. First, patches of wild-type cells visible in the eyes reflect groups of cells in the eye in which there was no mutagenesis. Second, uniform colored-eyed phenotypes may arise as a consequence of the kynurenine hydroxylase enzyme being diffusible throughout the insect (28), in which case the colored eyes could arise from patches of wild-type cells outside the eye contributing enough enzyme to produce some pigment in the eyes. Alternatively, NHEJ may generate partial loss-of-function alleles whose products synthesize reduced levels of pigment.

An observation that does not have a straightforward explanation is the difference in inheritance seen in the G_2 progeny of the original 10.1 and 10.2 G_1 founder males. One male founder (10.1) transmitted the construct to all of its G_2 progeny, whereas the other (10.2) transmitted the element in a Mendelian fashion. The insertion events of both of these males are precise based on sequencing of junction fragments in genomic DNA. Furthermore, the G_2 progeny of these males efficiently propagated the cargo to G_3 male and female progeny, indicating that both insertional events had functional converting elements. Because DsRed$^+$ G_2 10.2 males and females transmitted the cargo at the same high frequency as their G_2 10.1 DsRed$^+$ counterparts, the differences in transmission observed between the two G_1 founders did not result in heritable differences in the transgene or its insertion site. It is possible that short-duration epigenetic differences between the two insertional events or differential persistence of injected Cas9 dsRNA may account for the observed transgene inheritance. The recovery of DsRed$^-$/kh^{w-} G_4 progeny from DsRed$^+$/kh^{w-} females is consistent with transgenerational perdurance of Cas9–gRNA complexes.

A number of alternate approaches could mitigate the maternal effects that result in a high frequency of NHEJ and drive-resistant loci. The most straightforward solution is to drive Cas9 with a male germ-line–specific *cis*-regulatory sequence such as those of the well-characterized β2-tubulin gene, which is expressed only in the sperm of dipterans including *D. melanogaster* (34–36), *An. stephensi* (37), and *Ae. aegypti* (38). Alternatively, it may be possible to reduce the activity of Cas9 in the egg by maternal (but not germ-line) expression of Cas9 and/or Ku70 RNAi constructs. This is similar to the approach applied here for the initial recovery of the AsMCRkh2 transgenic mosquitoes. Advances in CRISPR/Cas9 research also offer potential solutions that greatly reduce the inhibition of HDR by the prior action of NHEJ by exploiting modified nucleases that cleave DNA at a distance from the gRNA recognition sequence, thereby allowing multiple rounds of target mutagenesis without eliminating the gRNA target site (39), or those that are mutated to cleave a single strand, the so-called nicking endonucleases (40). Autonomous gene-drive constructs using these modified nucleases may be less susceptible to NHEJ alteration of the homologous chromosome, which could then remain an efficient target for subsequent HDR-mediated conversion in the germ line. Future tests of these various strategies should establish those approaches that are the most effective for robust multigenerational maintenance of gene drive.

Gene-drive systems for population modification of vector mosquitoes have been proposed for nearly half a century (41). The phenomenal rate of allelic conversion achieved is a milestone achievement in the development of population-modification strategies for controlling malaria and other vector-borne diseases. These efforts justify a degree of optimism for the future successful application of this technology. We are fully aware that much needs to be done before laboratory achievements of this type are moved to the field. Effector gene stability in different genetic backgrounds and under diverse environmental conditions and efficacy against genetically diverse parasites need further research to ensure that the constructs function as well in the field as they do in the laboratory. In addition, significant advances in regulatory structures and ethical models of community engagement are as important as the further scientific development of these technologies (7, 42, 43). It is incumbent on the scientist developing these technologies to interact openly and freely with the potential end users. Finally, we do not believe that these technologies alone will be sufficient for malaria eradication. We support the combined efforts of people developing prophylactic and therapeutic drugs, vaccines, and alternate vector-control measures.

Materials and Methods

Mosquito Rearing and Maintenance. A colony of *An. stephensi* (15) bred in our insectary for >7 y was used in the experiments. The mosquitoes were maintained at 27 °C with 77% humidity and a 12-h day/night, 30-min dusk/dawn lighting cycle. Larvae were fed a diet of powdered fish food (Tetra-Min) mixed with yeast. Adults were provided with water and a 10% (wt/vol) sucrose solution ad libitum. Blood meals were provided by artificial feeding or mice. Protocols were approved by the Intuitional Animal Care and Use Committee of the University of California, Irvine (NIH Animal Welfare Assurance no. A3416.01). Mosquito containment followed recommended procedures (44).

Oligonucleotide Primers. *SI Appendix*, Table S2 lists oligonucleotide primer names and sequences used for gene amplification.

Design of the Gene-Drive Construct. Standard molecular biological procedures were used to construct the gene-drive plasmid, pAsMCRkh2. Detailed descriptions of the construction and plasmid architecture are provided in *SI Appendix, Materials and Methods*.

Generation of Double-Stranded RNA. Double-stranded RNA was generated to inhibit the expression of Cas9 from the donor plasmid during microinjection. Previous injections using Cas9 expressed from a plasmid or from Cas9 mRNA were unsuccessful, and we hypothesized that a high amount of Cas9 could be toxic to the embryos. Therefore, a total of 100 ng/μL Cas9 protein was included in the injection mixture along with dsRNA targeting Cas9 mRNA so that Cas9 mRNA generated by expression from the donor plasmid in the embryo would be destroyed and only the injected protein would be present. Additionally, dsRNA was injected targeting the putative ortholog of Ku70, a protein essential for nonhomologous end joining (45, 46). Knockdown of this protein may increase the possibility of repair by homologous recombination (47, 48). The putative ortholog for Ku70 in *An. stephensi*, ASTE011109, was identified by homology to *Bombyx mori* X-ray repair cross-complementing protein 5-like mRNA (LOC101736121) using the BLAST tool available at VectorBase.org. Primers were designed to amplify a 561-bp region of the ASTE011109 transcript and a 637-bp region of the *An. stephensi* codon-optimized Cas9, such that the amplicons did not contain >19 bp of identity to any other putative transcript available on VectorBase to avoid off-target effects. Both forward and reverse primers have T7 promoters at the 5′ end. The amplification products were purified using DNA Clean & Concentrator (Zymo) and used as a template for reverse transcription using the RNAi Kit from Ambion.

Microinjection and Screening Procedures. Microinjections were performed as described previously (10). Embryos were injected with a solution containing 100 ng/μL each of the plasmid, pAsMCRkh2, Cas9 protein, Cas9 dsRNA, and Ku70 dsRNA. G_0 males and females were outcrossed to wild-type mosquitoes in pools of ∼5 G_0 males or 15–30 G_0 females. All G_1, G_2, G_3, and G_4 progeny were screened as larvae for DsRed fluorescence under UV-fluorescence microscopy, and adults were screened under light microscopy.

RT-PCR. RT-PCR analyses were adapted from those used in ref. 11 with an additional RNA purification with Zymo RNA Clean & Concentrator. A total of 15 males and 30 female carcasses and dissected midguts from mixed heterozygous and homozygous DsRed$^+$ G_3 mosquitoes was used for each RNA preparation. Two hundred nanograms of DNase-treated total RNA was used in each reaction.

ACKNOWLEDGMENTS. The authors are grateful to Judy Coleman and Thai Binh Pham for mosquito husbandry. Research was supported by grants from the NIH (AI070654 and NS029870), a generous gift from Drs. Sarah Sandell and Michael Marshall (to E.B.), the W. M. Keck Foundation, and the NIH National Institute of Allergy and Infectious Diseases (AI29746 and AI116433 to A.A.J.).

1. White NJ, et al. (2014) Malaria. *Lancet* 383(9918):723–735.
2. World Health Organization (2014) *World Malaria Report, 2013* (WHO, Geneva, Switzerland).
3. World Health Organization (2015) *World Malaria Report, 2014* (WHO, Geneva, Switzerland).
4. Nájera JA (2001) Malaria control: Achievements, problems and strategies. *Parassitologia* 43(1-2):1–89.
5. malERA Consultative Group on Vector Control (2011) A research agenda for malaria eradication: Vector control. *PLoS Med* 8(1):e1000401.
6. Luckhart S, Lindsay SW, James AA, Scott TW (2010) Reframing critical needs in vector biology and management of vector-borne disease. *PLoS Negl Trop Dis* 4(2):e566.
7. Macias VM, James AA (2015) Impact of genetic modification of vector populations on the malaria eradication agenda. *Genetic Control of Malaria and Dengue*, ed Adelman ZN (Elsevier Academic, San Diego), pp 423–444.
8. Collins FH, James AA (1996) Genetic modification of mosquitoes. *Sci Med* 3(6):52–61.
9. James AA, et al. (1999) Controlling malaria transmission with genetically-engineered, *Plasmodium*-resistant mosquitoes: Milestones in a model system. *Parassitologia* 41(1-3):461–471.
10. Isaacs AT, et al. (2011) Engineered resistance to *Plasmodium falciparum* development in transgenic *Anopheles stephensi*. *PLoS Pathog* 7(4):e1002017.
11. Isaacs AT, et al. (2012) Transgenic *Anopheles stephensi* coexpressing single-chain antibodies resist *Plasmodium falciparum* development. *Proc Natl Acad Sci USA* 109(28):E1922–E1930.
12. Ito J, Ghosh A, Moreira LA, Wimmer EA, Jacobs-Lorena M (2002) Transgenic anopheline mosquitoes impaired in transmission of a malaria parasite. *Nature* 417(6887): 452–455.
13. Corby-Harris V, et al. (2010) Activation of Akt signaling reduces the prevalence and intensity of malaria parasite infection and lifespan in *Anopheles stephensi* mosquitoes. *PLoS Pathog* 6(7):e1001003.
14. James AA, Peloquin JJ (1998) Engineering resistance to malaria parasite development in mosquitoes. *Malaria: Parasite Biology, Pathogenesis and Protection*, ed Sherwin IW (ASM, Washington, DC), pp 63–69.
15. Jiang X, et al. (2014) Genome analysis of a major urban malaria vector mosquito, *Anopheles stephensi*. *Genome Biol* 15(9):459.
16. Sharma VP (1999) Current scenario of malaria in India. *Parassitologia* 41(1-3):349–353.
17. Gakhar SK, Sharma R, Sharma A (2013) Population genetic structure of malaria vector *Anopheles stephensi* Liston (Diptera: Culicidae). *Indian J Exp Biol* 51(4):273–279.
18. Murray CJ, et al. (2012) Global malaria mortality between 1980 and 2010: A systematic analysis. *Lancet* 379(9814):413–431.
19. Faulde MK, Rueda LM, Khaireh BA (2014) First record of the Asian malaria vector *Anopheles stephensi* and its possible role in the resurgence of malaria in Djibouti, Horn of Africa. *Acta Trop* 139:39–43.
20. Catteruccia F, et al. (2000) Stable germline transformation of the malaria mosquito *Anopheles stephensi*. *Nature* 405(6789):959–962.
21. Amenya DA, et al. (2010) Comparative fitness assessment of *Anopheles stephensi* transgenic lines receptive to site-specific integration. *Insect Mol Biol* 19(2):263–269.
22. Hollingdale MR, Nardin EH, Tharavanij S, Schwartz AL, Nussenzweig RS (1984) Inhibition of entry of *Plasmodium falciparum* and *P. vivax* sporozoites into cultured cells; an in vitro assay of protective antibodies. *J Immunol* 132(2):909–913.
23. Li F, Patra KP, Vinetz JM (2005) An anti-Chitinase malaria transmission-blocking single-chain antibody as an effector molecule for creating a *Plasmodium falciparum*-refractory mosquito. *J Infect Dis* 192(5):878–887.
24. Robert MA, Okamoto KW, Gould F, Lloyd AL (2014) Antipathogen genes and the replacement of disease-vectoring mosquito populations: A model-based evaluation. *Evol Appl* 7(10):1238–1251.
25. Klassen W, Curtis CF (2005) History of the sterile insect technique. *Sterile Insect Technique: Principles and Practice in Area-Wide Integrated Pest Management*, eds Dyck VA, Hendrichs J, Robinson AS (Springer Dordrecht, The Netherlands), pp 3–36.
26. Gantz VM, Bier E (2015) Genome editing. The mutagenic chain reaction: A method for converting heterozygous to homozygous mutations. *Science* 348(6233):442–444.
27. Bhalla SC (1968) White eye, a new sex-linked mutant of *Aedes aegypti*. *Mosq News* 28(3):380–385.
28. Han Q, et al. (2003) Analysis of the wild-type and mutant genes encoding the enzyme kynurenine monooxygenase of the yellow fever mosquito, *Aedes aegypti*. *Insect Mol Biol* 12(5):483–490.
29. Aryan A, Anderson MA, Myles KM, Adelman ZN (2013) TALEN-based gene disruption in the dengue vector *Aedes aegypti*. *PLoS One* 8(3):e60082.
30. Horn C, Wimmer EA (2000) A versatile vector set for animal transgenesis. *Dev Genes Evol* 210(12):630–637.
31. Basu S, et al. (2015) Silencing of end-joining repair for efficient site-specific gene insertion after TALEN/CRISPR mutagenesis in *Aedes aegypti*. *Proc Natl Acad Sci USA* 112(13):4038–4043.
32. Papathanos PA, Windbichler N, Menichelli M, Burt A, Crisanti A (2009) The vasa regulatory region mediates germline expression and maternal transmission of proteins in the malaria mosquito *Anopheles gambiae*: A versatile tool for genetic control strategies. *BMC Mol Biol* 10:65.
33. Nirmala X, et al. (2006) Functional characterization of the promoter of the vitellogenin gene, AsVg1, of the malaria vector, *Anopheles stephensi*. *Insect Biochem Mol Biol* 36(9):694–700.
34. Kemphues KJ, Kaufman TC, Raff RA, Raff EC (1982) The testis-specific beta-tubulin subunit in *Drosophila melanogaster* has multiple functions in spermatogenesis. *Cell* 31(3 Pt 2):655–670.
35. Michiels F, Gasch A, Kaltschmidt B, Renkawitz-Pohl R (1989) A 14 bp promoter element directs the testis specificity of the *Drosophila* beta 2 tubulin gene. *EMBO J* 8(5): 1559–1565.
36. Santel A, Kaufmann J, Hyland R, Renkawitz-Pohl R (2000) The initiator element of the *Drosophila* beta2 tubulin gene core promoter contributes to gene expression in vivo but is not required for male germ-cell specific expression. *Nucleic Acids Res* 28(6): 1439–1446.
37. Catteruccia F, Benton JP, Crisanti A (2005) An *Anopheles* transgenic sexing strain for vector control. *Nat Biotechnol* 23(11):1414–1417.
38. Smith RC, Walter MF, Hice RH, O'Brochta DA, Atkinson PW (2007) Testis-specific expression of the beta2 tubulin promoter of *Aedes aegypti* and its application as a genetic sex-separation marker. *Insect Mol Biol* 16(1):61–71.
39. Zetsche B, et al. (2015) Cpf1 is a single RNA-guided endonuclease of a class 2 CRISPR-Cas system. *Cell* 163(3):759–771.
40. Cong L, et al. (2013) Multiplex genome engineering using CRISPR/Cas systems. *Science* 339(6121):819–823.
41. Curtis CF (1968) Possible use of translocations to fix desirable genes in insect pest populations. *Nature* 218(5139):368–369.
42. Benedict M, et al. (2014) *Guidance Framework for Testing of Genetically Modified Mosquitoes* (WHO/TDR, Geneva, Switzerland).
43. Brown DM, Alphey LS, McKemey A, Beech C, James AA (2014) Criteria for identifying and evaluating candidate sites for open-field trials of genetically engineered mosquitoes. *Vector Borne Zoonotic Dis* 14(4):291–299.
44. Akbari OS, et al. (2015) Safeguarding gene drive experiments in the laboratory. *Science* 349(6251):927–929.
45. Lieber MR (2010) The mechanism of double-strand DNA break repair by the nonhomologous DNA end-joining pathway. *Annu Rev Biochem* 79:181–211.
46. Williams GJ, et al. (2014) Structural insights into NHEJ: Building up an integrated picture of the dynamic DSB repair super complex, one component and interaction at a time. *DNA Repair (Amst)* 17:110–120.
47. Adelman ZN, et al. (2007) nanos gene control DNA mediates developmentally regulated transposition in the yellow fever mosquito *Aedes aegypti*. *Proc Natl Acad Sci USA* 104(24):9970–9975.
48. Ma S, et al. (2014) CRISPR/Cas9 mediated multiplex genome editing and heritable mutagenesis of BmKu70 in *Bombyx mori*. *Sci Rep* 4:4489.

Supporting Information Appendix

Table S1. Larval and adult phenotypes of G_2 progeny of lines 10.1 and 10.2 G_1 outcrosses to wild-type mosquitoes.

G_1 Founder	Larval phenotypes*				Adult phenotypes*							
					Males				Females			
	$DsRed^+/kh^{w+}$	$DsRed^+/kh^{w-}$	$DsRed/kh^{w+}$	$DsRed^-/kh^{w-}$	$DsRed^+/kh^{w+}$	$DsRed^+/kh^{w-}$	$DsRed^-/kh^{w+}$	$DsRed^-/kh^{w-}$	$DsRed^+/kh^{w+}$	$DsRed^+/kh^{w-}$	$DsRed^-/kh^{w+}$	$DsRed/kh^{w-}$
10.1 ♂	16				6				8			
10.2 ♂	64		76		32		38		25		34	

*Shaded cells are G_2 progeny positive for DsRed ($DsRed^+$).

Table S2. List of oligonucleotide primers.*

Primer	Sequence (5'-3')	Reference
Vg451	GTACGCGTATCGATAAGCTTtaaGATACATTGATGAGTTTGG	This study
Vg452	TAGGCCGGCCGATCTCGGATCTGACAATG	This study
Vg453	GCTTATCGATACGCGTACGCATCTGCATCCTGGTACCACAGTCTTATTGG	This study
Vg454	GTACTTCTTATCCATCTTCCTAGATCGATTTTAAGCACGCCGC	This study
Vg455	CTAGGAAGATGGATAAGAAGTACTCGATCGGTCTGGATATCGG	This study
Vg456	CTCTCGTTACACCTTGCGCTTCTTCTTCGGCG	This study
Vg457	GCAAGGTGTAACGAGAGTTCGGTGCGAATCTCTCTCTTGATTTTTCCC	This study
Vg458	AGATCGGCCGGCCTAACCAAGGCCAGCCTGTTGAGC	This study
Vg464	AAGCTTATCGATACGCGTACCTCAACTGCCGACGAGTTGCTCG	This study
Vg465	ATCCGAGATCGGCCGGCCTACGTTCTGCGTGGCTGTTGTAAGGTTCC	This study
Vg494	GGTATCAGCTCACTCAAAGGCGGTAATACGG	This study
Vg495	GAAAGGGCCTCGTGATACGCCTATTTTTATAGG	This study
Vg498	CCTTTGAGTGAGCTGATACCCCCAAAAATTGACCTCAGATCTCTCAAGAAGCG	This study
Vg499	GCGTATCACGAGGCCCTTTCGCATCTGAACGAGGTGCTGCTAAATGG	This study
Vg500	GTTTTAGAGCTAGAAATAGCAAGTTAAAATAAGGCTAGTCCGTTATCAACTTGAAAAAGTGGCAC CGAGTCGGTGCTTTTTTTGTGGAAATTTGATTCACTTGTTTTAGG	This study
Vg501	AGGTCTTCTCGAAGACCCCAAGGGAGGGGGCAAATGGGTTGG	This study
Vg505	GTCCACTAACGAAAGAGGTCAAGAGC	This study
Vg507	CGATCGTTTAGTGACGAGATCACGC	This study
Vg537	CTTGATGGTTCCGTTCTACGGGC	This study
Vg538	AAACGCCCGTAGAACGGAACCAT	This study
Vg543	CATGTACATTTCCTTTTACGttaattaaCGTAGAACGGAACCATCGCGTGC	This study
Vg544	ATGGTTCCGTTCTACGttaattaaCGTAAAAGGAAATGTACATGGTAAAGCAATCTGACG	This study
Vg546	CCGGGCGAGCTCGactcgagcCTGGTACCACAGTCTTATTGGCGTGATGG	This study
Vg551	CAATAAGACTGTGGTACCAGgctcgagTTGTTTGATCGCACGGTTCCCACAATGG	This study
Vg552	CCTTACAACAGCCACGCAGAACGggatccGGCAGGGCATGAACGCGGGCTTTGAAGAC	This study
Vg553	GCCCGCGTTCATGCCCTGCCggatccCGTTCTGCGTGGCTGTTGTAAGGTTTCG	This study
Vg554	GCTCAACAGGCTGGCCTTGGTActcgagCTCAACTGCCGACGAGTTGCTCG	This study
Vg555	CAACTCGTCGGCAGTTGAGctcgagTACCAAGGCCAGCCTGTTGAGCAGCTTGC	This study
Vg557	CGATCGTTTAGTGACGAGATCACGC	This study
dsCas9 1 F	TAATACGACTCACTATAGTGCCATCCTGCTGTCGGATA	This study
dsCas9 1 R	TAATACGACTCACTATAGCTTCGGCAGCACCTTCTCGT	This study
dsKu70 F	TAATACGACTCACTATAGCTACGGCATTGGGTTTGTCT	This study
dsKu70 R	TAATACGACTCACTATAGGCTTAGCTTGTAGCCGGATG	This study
G1F2	CGTATGCTGCACGACGTTAAC	This study

G2R1	CTGGACATCTGCTTCTGAG	This study
G2R2	GCAATAGCTGACTCCTG	This study
Km1F1	CGATGCGATCGAGCTAATTG	This study
Km2R1	GTGACGAGATCACGCATCTG	This study
Vg5'R1	CGTTTGGTGCTCAGCTCAGAC	This study
Vg5'R2	GTCGTAGGTGGTGGTATGCTAAC	This study
U6F1	CTACCTGTACGATGGCTTAAG	This study
m2A10 FOR	GAGACGGTGAAGATCTCGTGCAAGG	1
m2A10 REV	GCTTCGTACCACCACCGAACACGTA	1
m1C3 FOR	AAGGGCTCGCTGAAACTGT	1
m1C3 REV	ACAGAAGTACACCGCCAGGT	1
AsVg1 for	CAACATCATGTCCAAGTCGGAGGTGA	2
AsVg1 rev	CTTGAAGCTTTCGTGCTCTTCCTCCG	2
AsCPAFOR	CTTTACGGAAACGCTCGAAG	3
AsCPAREV	CCATAGCAGAATGGACCGTAA-3′	3
Asrib26Sfor	AATCCTTCCCGAAGGACATGAACCG	4
Asrib26Srev	TACGAAACAAATCCCATCCTAATCGAAGC	4

*Lowercase letters are introduced restriction endonuclease cleavage sites.

Table S3. G_3 larval phenotypes of line 10.1 G_2 outcrosses to wild-type mosquitoes.			
Founder[†]	**Cross**	**Larval phenotypes**[*]	
		DsRed$^+$	**DsRed**$^-$
♂	**10.1.1**	346	2
	10.1.3	136	
	10.1.5	129	1
	10.1.6	218	
	Subtotal[‡]	**829**	**3**
♀	**10.1.1**	61	1
	10.1.2	109	2
	10.1.3	48	1
	10.1.4	85	
	10.1.5	85	
	10.1.7	41	
	10.1.8	63	
	Subtotal[‡]	**492**	**4**
	Total	**1321**	**7**

[*]Shaded cells are G_3 progeny positive for DsRed (DsRed$^+$).
[†]Progeny of single G_2 male or female out-crossed to wild-types of the opposite sex.
[‡]X^2 analyses show significant differences (p<<0.0001) in DsRed$^+$:DsRed$^-$ ratios from random segregation.

Table S4. G_3 larval phenotypes of line 10.2 G_2 outcrosses to wild-type mosquitoes.				
Founder	**Cross**	**Larval phenotypes**[*]		
		DsRed$^+$	**DsRed**$^-$	**DsRed**$^-$**/kh**$^{w-}$
♀[†]	**10.2.3**	109		1
	10.2.4	141		
	10.2.5	82		
	10.2.6	100		
	10.2.8	163		1
	10.2.10	146		
	10.2.11	90		
	10.2.12	117	1	
	10.2.13	119		
	10.2.14	70		
	10.2.15	9	1	
	10.2.16	89	7	
	10.2.17	131	1	
	10.2.18	112		1
	10.2.19	93		
	Subtotal[§]	**1571**	**10**	**3**
♂[‡]	**Batch**[§]	**3060**	**25**	
	Total[§]	**4631**	**35**	**3**

[*]Shaded cells are G_3 progeny positive for DsRed (DsRed$^+$).
[†]Progeny of single G_2 female out-crossed to wild-type males.
[‡]27 G_2 males out-crossed to 270 wild-type females.
[§]X^2 analyses show significant differences (p<<0.0001) in DsRed$^+$:DsRed$^-$ ratios from random segregation.

Table S5. G_3 adult phenotypes of line 10.1 G_2 outcrosses to wild-type mosquitoes.

Founder[†]	Cross	Adult phenotypes[*]									
		Males					Females				
		DsRed$^+$/kh^{w+}	DsRed$^+$/kh^{w-}	DsRed$^+$/ mosaic	DsRed$^-$/kh^{w+}	DsRed$^-$/kh^{w-}	DsRed$^+$/kh^{w+}	DsRed$^+$/kh^{w-}	DsRed$^+$/ mosaic	DsRed$^-$/kh^{w+}	DsRed$^-$/kh^{w-}
♂	**10.1.1**	202			2		173				
	10.1.3	54					91				
	10.1.5	58			1		53				
	10.1.6	100					102				
	Total[‡]	**414**			**3**		**419**				
♀	**10.1.1**		20	7	1			18	7		
	10.1.2		26	4				36	4	2	
	10.1.3		9	3				15	3		
	10.1.4		26					32	4		
	10.1.5		38	7				37	7		
	10.1.7		13	2				19			
	10.1.8		23	2				23	2		
	Total[‡]		**155**	**25**	**1**			**180**	**27**	**2**	

[*]Shaded cells are G_3 progeny positive for DsRed (DsRed$^+$).
[†]Progeny of single G_2 male or female out-crossed to wild-types of the opposite sex.
[‡]X^2 analyses show significant differences ($p<<0.0001$) in DsRed$^+$:DsRed$^-$ ratios from random segregation.

Table S6. G_3 adult phenotypes of line 10.2 G_2 outcrosses to wild-type mosquitoes.

Founder	Cross	Adult phenotypes*									
		Males					Females				
		$DsRed^+/kh^{w+}$	$DsRed^+/kh^{w-}$	$DsRed^+$/mosaic§		$DsRed^-/kh^{w+}$	$DsRed^-/kh^{w-}$	$DsRed^+/kh^{w+}$	$DsRed^+/kh^{w-}$	$DsRed^+$/mosaic§		$DsRed^-/kh^{w+}$	$DsRed^-/kh^{w-}$
♀†	**10.2.3**		66	5	ND				44		ND		
	10.2.4		64		ND				61		ND		
	10.2.5		36	7	ND				32	3	ND		
	10.2.6		36	2	ND				33		ND		
	10.2.8		60		ND				51		ND		
	10.2.10		48	2	20				49	3	14		
	10.2.11		30	1	8				41	2	4		
	10.2.12		36	3	10				38	3	7		
	10.2.13		38	2	7				42	2	1		
	10.2.14		22	1	7				29	2	3		
	10.2.15		4		2				2				
	10.2.16		42	1	1				37		3		
	10.2.17		38	6	20				44	1	19		
	10.2.18		40	4	7				48	3	1		
	10.2.19		37	5	9				34	4	4		
	Total¶		**597**	**130**					**585**	**79**			
♂‡	**Batch¶**	**663**				**8**		**595**				**8**	

*Shaded cells are G_3 progeny positive for DsRed ($DsRed^+$).
†Progeny of single G_2 female out-crossed to wild-type males.
‡27 G_2 males out-crossed to 270 wild-type females.
§The first column numbers are those mosquitoes with mosaicism in the eye. The second column numbers are mosquitoes with the 'colored' eye phenotypes consistent with mosaicism in the rest of the body. 'ND', not determined.
¶X^2 analyses show significant differences ($p<<0.0001$) in $DsRed^+$:$DsRed^-$ ratios from random segregation.

Table S7. G_4 larval phenotypes of line 10.1 G_3 outcrosses to wild-type mosquitoes.		
(Cross)Transgenic parent (n) *	**Larval phenotypes**†	
	DsRed$^+$	**DsRed$^-$**
(1) DsRed$^+$/*kh*$^{w-}$ ♀ (26)	28	20
(2) DsRed$^+$/*kh*$^{w-}$ ♂ (32)	332	303
(5) DsRed$^+$/*kh*$^{w+}$ ♀ (40)‡	645	7
(6) DsRed$^+$/*kh*$^{w+}$ ♂ (40)‡	949	6

*Progeny of batch-mated G_3 males or females out-crossed to wild-types of the opposite sex. (n) is the number of transgenic founder parents.
†Shaded cells are G_4 progeny positive for DsRed (DsRed$^+$).
‡X^2 analyses show significant differences (p<<0.0001) in DsRed$^+$:DsRed$^-$ ratios from random segregation.

Table S8. G_4 larval phenotypes of line 10.2 G_3 outcrosses to wild-type mosquitoes.		
(Cross)Transgenic parent (n)*	**Larval phenotypes**†	
	DsRed$^+$	**DsRed$^-$**
(3) DsRed$^+$/*kh*$^{w-}$ ♀ (43)	204	120
(4) DsRed$^+$/*kh*$^{w-}$ ♂ (25)	372	260
(7) DsRed$^+$/*kh*$^{w+}$ ♀ (50)‡	1134	20
(8) DsRed$^+$/*kh*$^{w+}$ ♂ (50)‡	609	19

*Progeny of batch-mated G_3 males or females out-crossed to wild-types of the opposite sex. (n) is the number of transgenic founder parents.
†Shaded cells are G_4 progeny positive for DsRed (DsRed$^+$).
‡X^2 analyses show significant differences (p<<0.0001) in DsRed$^+$:DsRed$^-$ ratios from random segregation .

Table S9. Table S9. G_4 larval phenotypes of lines 10.1 and 10.2 batch G_3 intercrosses.[1]		
	Larval phenotypes†	
Cross	**DsRed$^+$/*kh*$^{w-}$**	**DsRed$^-$/*kh*$^{w-}$**
Line 10.1	428	71
Line 10.2	1851	361

[1]G_3 DsRed-positive (DsRed$^+$) males and females were intercrossed as a single batch for each line.
†Shaded cells are G_4 progeny positive for DsRed (DsRed$^+$).

Table S10. G_4 adult phenotypes of line 10.1 G_3 outcrosses to wild-type mosquitoes.

Line	(Cross) Founder	Adult phenotypes[1]									
		G_4 males					G_4 females				
		DsRed$^+$/ kh^{w+}	DsRed$^+$/ kh^{w-}	DsRed$^+$/ mosaic†		DsRed$^-$/ kh^{w+}	DsRed$^-$/ kh^{w-}	DsRed$^+$/ kh^{w+}	DsRed$^+$/ kh^{w-}	DsRed$^+$/ mosaic†		DsRed$^-$/ kh^{w+}	DsRed$^-$/ kh^{w-}
10.1	(1) DsRed$^+$/*kh*$^{w-}$ ♀		6		5	4	3		1	3	4	7	2
	(2) DsRed$^+$/*kh*$^{w-}$ ♂‡	153				111		153				137	
	(5) DsRed$^+$/*kh*$^{w+}$ ♀§	1	155	13	85	5	1		223	19	71	4	
	(6) DsRed$^+$/*kh*$^{w+}$ ♂§	403				3		479				3	

*Shaded cells are G_4 progeny positive for DsRed (DsRed$^+$).

†The first column numbers are those mosquitoes with mosaicism in the eye. The second column numbers are mosquitoes with the 'colored' eye phenotypes consistent with mosaicism in the rest of the body.

‡X^2 analyses show significant differences (p=0.0137) in DsRed$^+$:DsRed$^-$ ratios from random segregation .

§ X^2 analyses show significant differences (p<<0.0001) in DsRed$^+$:DsRed$^-$ ratios from random segregation.

Table S11. G_4 adult phenotypes of line 10.2 G_3 outcrosses to wild-type mosquitoes.													
Line	(Cross) Founder	Adult phenotypes*											
		G_4 males						G_4 females					
		DsRed$^+$/ kh^{w+}	DsRed$^+$/ kh^{w-}	DsRed$^+$/ mosaic †		DsRed$^{-/}$ kh^{w+}	DsRed$^-$/ kh^{w-}	DsRed$^+$/ kh^{w+}	DsRed$^+$/ kh^{w-}	DsRed$^+$/ mosaic †		DsRed$^{-/}$ kh^{w+}	DsRed$^-$/ kh^{w-}
10.2	(3) DsRed$^+$/*kh*$^{w-}$ ♀‡		40	1	34	36	41		41		53	23	3
	(4) DsRed$^+$/*kh*$^{w-}$ ♂§	157				101		160				139	
	(7) DsRed$^+$/*kh*$^{w+}$ ♀¶	3	288	8	120	5		1	357	16	145		3
	(8) DsRed$^+$/*kh*$^{w+}$ ♂¶	258				10		307				8	

*Shaded cells are G_4 progeny positive for DsRed (DsRed$^+$).

†The first column numbers are those mosquitoes with mosaicism in the eye. The second column numbers are mosquitoes with the 'colored' eye phenotypes consistent with mosaicism in the rest of the body.

‡X^2 analyses show significant differences ($p<0.0001$) in DsRed$^+$:DsRed$^-$ ratios from random segregation.

§X^2 analyses show significant differences ($p=0.0011$) in DsRed$^+$:DsRed$^-$ ratios from random segregation.

¶X^2 analyses show significant differences ($p<<0.0001$) in DsRed$^+$:DsRed$^-$ ratios from random segregation.

Figure S1. Molecular confirmation of the precise insertions of the AsMCRkh2 cargo into the *kh*^{w} locus. Sequencing of the 5'- and 3'-end G1F2-vg5'1 and U6F1-G2R2 junction amplification fragments (left and right, respectively) amplified from the G_1 founder male mosquitoes 10.1 and 10.2 (lower sequencing traces) revealed a perfect match to the sequences from Cas9-mediated cleavage at the kh2 target site and precise integration of the ASMCRkh2 cargo (Figure 1) into that site. Positions of the kh2 homology arms (maroon boxes), guide RNA targeting sequences (blue boxes), PAM site (red arrowhead) and the PCR primers Vg-5prime (orange box) and U6A3'Seq (red box) are shown. Genomic nucleotides depicted in lower case letters indicate restriction endonuclease enzyme recognition sites used in the construction of the AsMCRkh2 cargo.

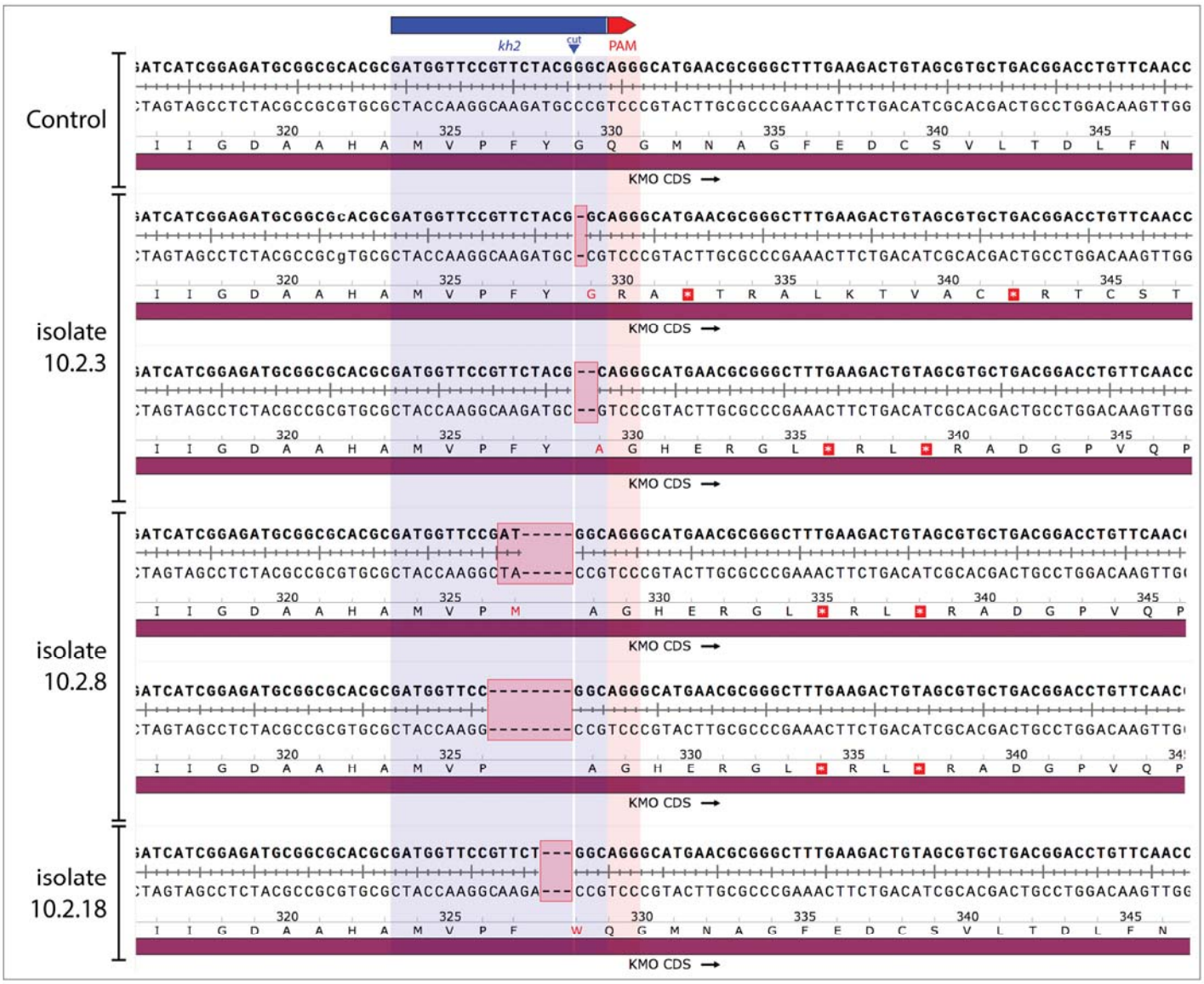

Figure S2. Mutated sequences at the kh2 target site in selected G_2 transgenic mosquitoes. The top sequence is the wild-type reference sequence at the kh2 target site from a control mosquito. The PAM sequence is shaded in peach, the 20 nt targeting sequence is shaded in purple, indels are shaded in pink, and the gRNA directed cleavage site by a thin vertical white line. NHEJ events were detected in three different white-eyed DsRed$^-$ mosquitoes. Different sequences were isolated by cloning PCR products generated from the *kh*^{w} locus in lines 10.2.3 and 10.2.8, supporting the conclusion that these mosquitoes are mosaics carrying at least two distinct NHEJ-directed mutations. Isolate 10.2.18 is derived from a direct sequencing reaction of an amplification product confirming that this transgenic mosquito had only a single NHEJ event. In contrast to the other two cases, this mutation maintains the translation frame but nonetheless results in a white-eye phenotype supporting the conclusion that the deletion of a single amino acid (Y328) and substitution of its neighbor (G329W) eliminates or greatly reduces kynurenine hydroxylase enzymatic activity.

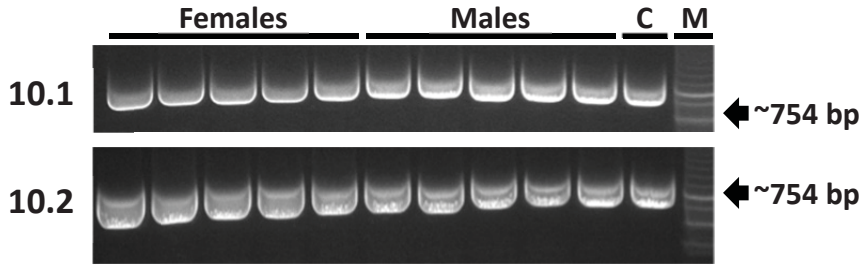

Figure S3. Gene amplification of the kh2 target sites in selected G_3 founder mosquitoes. Genomic DNA prepared from individual male and female G_3 founder mosquitoes positive for DsRed and with white eyes ($DsRed^+/kh^{w-}$; crosses 1 - 4, Tables S10 and S11) was used with the gene-specific primers, vg505 and vg557 (Table S2) to amplify a portion of the kh^w gene. The diagnostic fragment at 754 base-pairs indicates at least one of the chromosomes had a kh^w gene without the large ~17 kb transgene cargo insert. These alleles must be mutant because the eye phenotype of each mosquito from which the DNA was derived is white (kh^{w-}). 'C' is a control sample of DNA from a wild-type mosquito. 'M' are the molecular-weight markers.

Supporting Materials and Methods.

Construction of the *vasa*-Cas9 cassette.
The *Drosophila melanogaster vasa* gene and its *Anopheles gambiae* ortholog AGAP008578 (5) were used as BLAST search queries to identify the ASTE003241 gene as the putative unique *Anopheles stephensi* ortholog. A 4009 bp genomic fragment comprising the *Anopheles stephensi vasa* promoter and regulatory sequences preceding the predicted translational start site was amplified using oligonucleotides vg453/vg454. Four DNA fragments were then joined in the following order: 1) the *An. stephensi vasa* regulatory fragment; 2) a recoded Cas9 gene codon-optimized for translation in *Anopheles stephensi* (pUC57Kan-T7-AsCas9 (amplified with the oligonucleotides vg455/vg456); 3) a 1014bp fragment following the translational stop codon (TAA) of the ASTE003241 (amplified using the oligonucleotides vg457/458), 4) the backbone of the pBacDsRed plasmid (amplified using the oligonucleotides vg451/vg452). These four amplicons were purified, treated with the restriction enzyme *Dpn*I to remove methylated DNA and joined in a Gibson assembly (New England Biolabs, #E5510S) reaction to obtain the plasmid pVG160 (pVG160_pBacDsRed-attB_Aste-Vasa-Cas9).

Construction of the U6A-kh-gRNA cassette. A 923bp fragment spanning the annotated *Anopheles stephensi* U6-snRNA gene ASTE015697 was amplified using the oligonucleotides vg464/vg465, and the amplification product was cloned into pCR2.1-TOPO using a TA Topoisomerase Cloning Kit (Invitrogen, #450641). The resulting plasmid was used as a template for site-directed mutagenesis using the oligonucleotides vg500/vg501 thereby substituting the U6 transcript with a 2x*Bbs*I restriction site linker followed by the gRNA core sequence. The resulting plasmid (pVG145) serves as vector for one-step insertion of 20 bp gRNA guide sequences to generate complete gRNAs under the control of the *An. stephensi* U6 RNA polymerase-III promoter. pVG145 was cut with the restriction enzyme *Bbs*I and a linker generated by annealing the oligonucleotides vg537/vg538 was ligated to close the gap, the resulting plasmid (pVG163) expresses a gRNA targeting cleavage of the *kynurenine hydroxylase-white* (*kh*^{w}) coding sequence at the sequence "GATGGTTCCGTTCTAC**G/GG**CAGG"; the **bolded "GGG"** corresponds to the encoded glycine 329 of the *kh*^{w} gene product.

Construction of the homology arms backbone (pVG159). To minimize the final vector size, a minimal 1943 bp backbone fragment of pUC19 was amplified using vg494/vg495 and fused to a 2.4kb genomic fragment from the *An. stephensi kh*^{w} locus (amplified with vg498/vg499), using Gibson assembly, to yield the plasmid pVG159.

Construction of the pAsMCRkh construct. The final construct, pAsMCRkh, was assembled using restriction cloning in two steps. First, a three-way fusion was generated comprising: 1) a fragment containing the pUC19 plasmid backbone and the *kh*^{w} homology arms was amplified from pVG159 using vg543/vg552, which added *Pac*I and *Bam*HI restriction enzyme cut sites at the ends; 2) a 6.6kb DNA fragment including the 3xP3-DsRed eye marker and a dual-single chain (scFv) antibody cassette expressing m1C3 and m2A10 (1,3) and amplified with vg544/vg551, which added *Pac*I and P*sp*XI sites at the ends); and 3) the U6A-kh2-gRNA cassette (amplified from pVG163 using vg553/vg554, which added *Psp*XI and *Bam*HI sites at the ends). Each of the three fragments was cut with the respective restriction enzymes followed by treatment with *Dpn*I to remove the methylated templates, and ligated together to obtain the intermediate plasmid pVG165. In the second step, the two above fragments were joined. The vasa-Cas9 cassette was amplified from pVG160 (using vg546/vg555, which added *Psp*XI sites at both ends) and the obtained amplicon was cut with *Psp*XI and *Dpn*I, and then ligated to pVG165 linearized with *Psp*XI (and treated with calf intestinal alkaline phosphatase to obtain the final construct.

Reagents: all amplification steps were performed using Phusion High-Fidelity DNA Polymerase (for fragments <6kb, New England Biolabs, Cat.#M0530S) or Q5 High-Fidelity DNA Polymerase (for fragments >6kb, New England Biolabs, Cat.#M0491S). The enzymes mentioned were purchased from New England Biolabs: *Bam*HI-

HF (R3136S), *Bbs*I (R0539S), *Dpn*I (R0176S), *Pac*I (R0547S), *Psp*XI (R0656S), calf intestinal alkaline phosphatase (M0290S).

References

1. Isaacs, A.T., Li, F., Jasinskiene, N., Chen, X., Nirmala, X., Marinotti, O., Vinetz, J.M. and James, A.A. (2011) Engineered resistance to *Plasmodium falciparum* development in transgenic *Anopheles stephensi*. *PLoS Pathogens* 7(4): PMID: 21533066, PMCID: PMC3080844
2. Nirmala, X., Marinotti, O., Sandoval, J.M., Phin, S., Gakhar, S., Jasinskiene. N. and James, A.A. (2006) Functional characterization of the promoter of the vitellogenin gene, *AsVg1*, of the malaria vector, *Anopheles stephensi*. *Insect. Biochem. Molec. Biol.,* **36,** 694-700. PMID: 16935218
3. Isaacs, A.T., Jasinskiene, N., Tretiakov, M., Thiery, I., Zettor, A., Bourgouin, C. and James, A.A. (2012) Transgenic *Anopheles stephensi* co-expressing single-chain antibodies resist *Plasmodium falciparum* development. *Proc. Natl. Acad. Sci. USA*, **109**, E1922-E1930. PMID:22689959. *PNAS PLUS*, **109**, 11070-11071.
4. Chen, X., Marinotti, O., Whitman, L., Jasinskiene N., Romans, P and James A.A. (2007) The *Anopheles gambiae* vitellogenin gene (*VGT2*) promoter directs persistent accumulation of a reporter gene product in transgenic *Anopheles stephensi* following multiple blood meals. *Am. J. Trop. Med. Hygiene* **76**, 1118-1124. PMID 17556621
5. Papathanos, P.A., Windbichler, N., Menichelli, M., Burt A. and Crisanti, A. (2009) The vasa regulatory region mediates germline expression and maternal transmission of proteins in the malaria mosquito Anopheles gambiae: a versatile tool for genetic control strategies. BMC Mol Biol. 2009 Jul 2;10:65. doi: 10.1186/1471-2199-10-65. PMID:19573226